

Multiphoton Bloch-Siegert shifts and level-splittings in a three-level system

P L Hagelstein¹, I U Chaudhary²

¹ Research Laboratory of Electronics, Massachusetts Institute of Technology, Cambridge, MA 02139,USA

E-mail: plh@mit.edu

² Research Laboratory of Electronics, Massachusetts Institute of Technology, Cambridge, MA 02139,USA

E-mail: irfanc@mit.edu

Abstract. In previous work we studied the spin-boson model in the multiphoton regime, using a rotation that provides a separation between terms that contribute most of the level energies away from resonance, and terms responsible for the level splittings at the anticrossing. Here, we consider a generalization of the spin-boson model consisting of a three-level system coupled to an oscillator. We construct a similar rotation and apply it to the more complicated model. We find that the rotation provides a useful approximation to the energy levels in the multiphoton region of the new problem. We find that good results can be obtained for the level splittings at the anticrossings for resonances involving the lower two levels in regions away from accidental or low-order resonances of the upper two levels.

PACS numbers: 32.80.Bx,32.60.+i,32.80.Rm,32.80.Wr

Submitted to: *J. Phys. B: At. Mol. Opt. Phys.*

1. Introduction

In early studies of spin dynamics in magnetic fields, Bloch and Siegert considered the basic problem of the two-level system with a sinusoidal perturbation [1]. The perturbation increases the level separation (the Bloch-Siegert shift), and energy can be exchanged with the two-level system when the transition energy matches an odd multiple of $\hbar\omega_0$ (Bloch-Siegert resonances), where ω_0 is the oscillatory frequency. These effects have been studied with a dynamical Hamiltonian [1, 2] (the Rabi Hamiltonian), and also with a static Hamiltonian [3] (the spin-boson Hamiltonian) in which the two-level system and oscillator are modeled as coupled quantum systems. These models have been of interest over the years for applications to physical systems, including spin problems [1, 4, 5] and atoms in strong electromagnetic fields [2, 6, 7, 8]; and also as standard model problems on which new approximation methods can be tested [9, 10]. We have been interested in such problems in order to better understand energy exchange between quantum systems with highly mismatched characteristic energies.

In this work, we address a generalization of the spin-boson problem in which a three-level system is coupled to an oscillator. Our interest in this problem is focused primarily on the multiphoton regime, in which the characteristic energy of the oscillator is small compared to the available transition energies of the three-level system. While there exists a modest literature on coupled oscillator and three-level models [11, 12, 13, 14, 15], there does not appear to be available previous work relevant to the multiphoton region. The rotating wave approximation has been applied with success near low-order resonances [16, 17, 18, 19, 20, 21, 22], but one would not expect this approach to be helpful in the multiphoton region.

The replacement of the two-level system of the spin-boson problem by a three-level system in the generalization of the model considered here very much complicates the problem. The convenient mathematical machinery of the spin operators and Pauli matrices available for the spin-boson problem is now replaced by the less convenient SU(3) operators and Gell-Mann matrices [23], and the diagonalization of the three-level system now involves a cubic characteristic equation. There can occur in addition level crossing effects in the three-level system in which the middle level is pushed through one of the other levels. Faced with such difficulties, it is no surprise that the three-level version of the model has not received comparable attention as a workhorse problem in comparison with the simpler spin-boson problem.

Here, we propose to use the more complicated coupled oscillator and three-level

model to test an approximation scheme that appears to have worked well in the spin-boson problem [24], and also in the generalization to the spin-1 version of the spin-boson model [25]. In this approach, the two-level or three-level system is diagonalized directly, treating the oscillator operators parametrically. The rotation which accomplishes this produces weaker residual couplings when applied to the oscillator. This rotation was discussed early on for the spin-boson problem by Wagner [26]. In the multi-photon region, the energy levels of the full problem are well approximated away from resonance by simple averages over the parameterized diagonalized energy levels. We expect this also to be the case in the coupled oscillator and three-level system problem. In the first half of this paper, we develop the approximation explicitly and compare with exact results for a test problem, with the result that the approximation gives good results away from resonances. We found previously in the spin-boson model that we could understand the level splittings at resonance from a simple two basis state approximation using matrix elements of the residual interaction arising from the rotation of the oscillator. We are interested in whether this is also the case in the more complicated version of the problem under consideration here. In the second half of this paper, we develop the interaction terms explicitly and compare approximate level splittings with exact numerical results from a test problem. We find that the method works well for high-order resonances away from accidental or low-order resonances on other transitions.

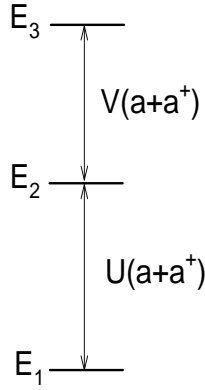


Figure 1. Three-level system and coupling.

2. Basic model and unitary transformation

The coupled oscillator and three-level system, which generalizes the spin-boson model, can be described using the Hamiltonian

$$\begin{aligned} \hat{H} = & \begin{pmatrix} E_1 & 0 & 0 \\ 0 & E_2 & 0 \\ 0 & 0 & E_3 \end{pmatrix} + \hbar\omega_0 \hat{a}^\dagger \hat{a} \\ & + U(\hat{a} + \hat{a}^\dagger) \begin{pmatrix} 0 & 1 & 0 \\ 1 & 0 & 0 \\ 0 & 0 & 0 \end{pmatrix} + V(\hat{a} + \hat{a}^\dagger) \begin{pmatrix} 0 & 0 & 0 \\ 0 & 0 & 1 \\ 0 & 1 & 0 \end{pmatrix} \end{aligned} \quad (1)$$

In this model, the three-level system has unperturbed energies E_1 , E_2 , and E_3 . Transitions between the first two levels are described by a linear coupling term, where the interaction has strength U . Transitions between the second and third levels are also included through another linear coupling term, with interaction strength V . Such a coupling scheme is normally called a ladder or a Ξ configuration [27]. We will also assume that

$$|E_i - E_j| \gg \hbar\omega_0, \quad n \gg 1$$

2.1. Rotation

In our earlier work, we used a unitary transformation to rotate the spin-boson Hamiltonian into a more complicated form which we wrote as

$$\hat{U}^\dagger \hat{H} \hat{U} = \hat{H}_0 + \hat{V} + \hat{W} \quad (2)$$

The rotation diagonalized the two-level model parameterized by the oscillator variable y defined as

$$y = \frac{\hat{a} + \hat{a}^\dagger}{\sqrt{2}} \quad (3)$$

Although the transformation introduced terms more complicated mathematically, the rotated Hamiltonian was conceptually simple. The first term \hat{H}_0 was found to produce a reasonably good approximation to the energy levels away from the anticrossings. The second term \hat{V} can be used to estimate the level splittings at the anticrossings. The third term \hat{W} is small in the large n regime, as is the case here.

2.2. Unperturbed rotated Hamiltonian \hat{H}_0

We focus first on \hat{H}_0 with the goal of developing an approximation for the energy levels away from the anticrossings. Following the approach used in the spin-boson version of the problem, the unitary transformation we use here is one which diagonalizes the part of the Hamiltonian that does not include the oscillator

$$\hat{H}_0 - \hbar\omega_0\hat{a}^\dagger\hat{a} = \hat{U}^\dagger \left(\hat{H} - \hbar\omega_0\hat{a}^\dagger\hat{a} \right) \hat{U} \quad (4)$$

Combining the different 3×3 matrices that appear in the Hamiltonian, we may write

$$\begin{aligned} \hat{H}_0 - \hbar\omega_0\hat{a}^\dagger\hat{a} &= \hat{U}^\dagger \begin{pmatrix} E_1 & \sqrt{2}Uy & 0 \\ \sqrt{2}Uy & E_2 & \sqrt{2}Vy \\ 0 & \sqrt{2}Vy & E_3 \end{pmatrix} \hat{U} \\ &= \begin{pmatrix} E_1(y) & 0 & 0 \\ 0 & E_2(y) & 0 \\ 0 & 0 & E_3(y) \end{pmatrix} \end{aligned} \quad (5)$$

2.3. Diagonalization

An explicit construction of the unitary transformation could be done for the simpler spin-boson problem, but this is inconvenient for the three-level version of the problem that we are interested in here. Nevertheless, we can still make progress by noting that the rotation accomplishes a diagonalization, which can be done by solving

$$\begin{pmatrix} E_1 & \sqrt{2}Uy & 0 \\ \sqrt{2}Uy & E_2 & \sqrt{2}Vy \\ 0 & \sqrt{2}Vy & E_3 \end{pmatrix} \begin{pmatrix} c_1 \\ c_2 \\ c_3 \end{pmatrix} = E(y) \begin{pmatrix} c_1 \\ c_2 \\ c_3 \end{pmatrix} \quad (6)$$

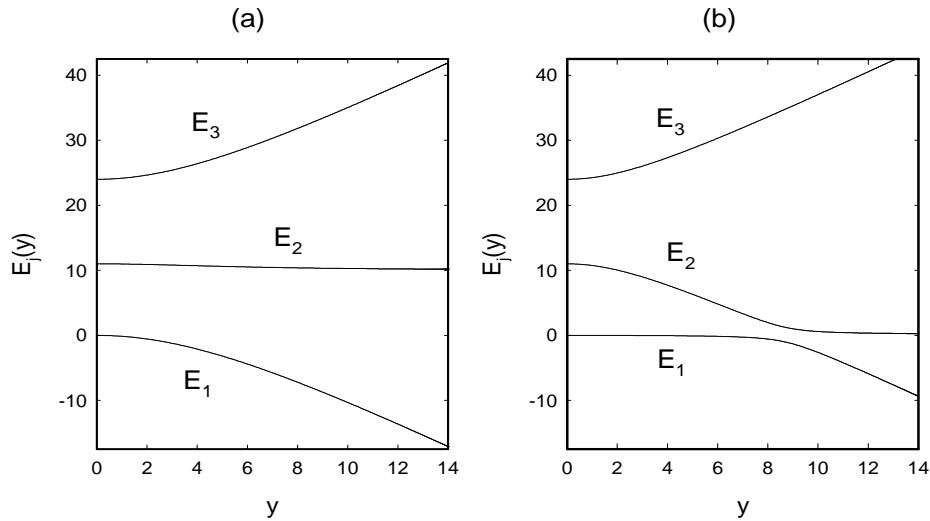


Figure 2. Energy levels $E_j(y)$ (in units of $\hbar\omega_0$) as a function of y for a model with $E_1 = 0$, $E_2 = 11 \hbar\omega_0$ and $E_3 = 24 \hbar\omega_0$. The number of oscillator quanta n is 10^8 . (a) The coupling strengths are $U\sqrt{n} = 0.8$ and $V\sqrt{n} = 0.8$. (b) The coupling strengths are $U\sqrt{n} = 0.1$ and $V\sqrt{n} = 1.0$.

This leads to a characteristic equation that is cubic

$$(E_1 - E)(E_2 - E)(E_3 - E) - (E_1 - E)2V^2y^2 - (E_3 - E)2U^2y^2 = 0 \quad (7)$$

We denote the solutions to this cubic equation as $E_1(y)$, $E_2(y)$ and $E_3(y)$, defined so that

$$E_1(0) = E_1 \quad E_2(0) = E_2 \quad E_3(0) = E_3$$

The solution of the cubic equation and expressions for the eigenvalues $E_j(y)$ are discussed in Appendix A. The unperturbed part of the rotated Hamiltonian \hat{H}_0 is then

$$\hat{H}_0 = \begin{pmatrix} E_1(y) & 0 & 0 \\ 0 & E_2(y) & 0 \\ 0 & 0 & E_3(y) \end{pmatrix} + \hbar\omega_0 \hat{a}^\dagger \hat{a} \quad (8)$$

2.4. Level crossing and anticrossing

The diagonalization of the three-level system parameterized by y produces energy levels that depend on y , examples of which are illustrated in Figure 2. We expect static coupling between levels to push them apart, and in the calculation of Figure 2(a) this is exactly what we see. However, since the interaction pushes levels apart, it is possible that one level may be pushed into and through another level. This is illustrated in

Figure 2(b), where the interaction between levels 2 and 3 is strong, and level one is weakly coupled. In this case level 2 anticrosses level 1. We refer to the middle level as $E_2(y)$ on either side of the anticrossing.

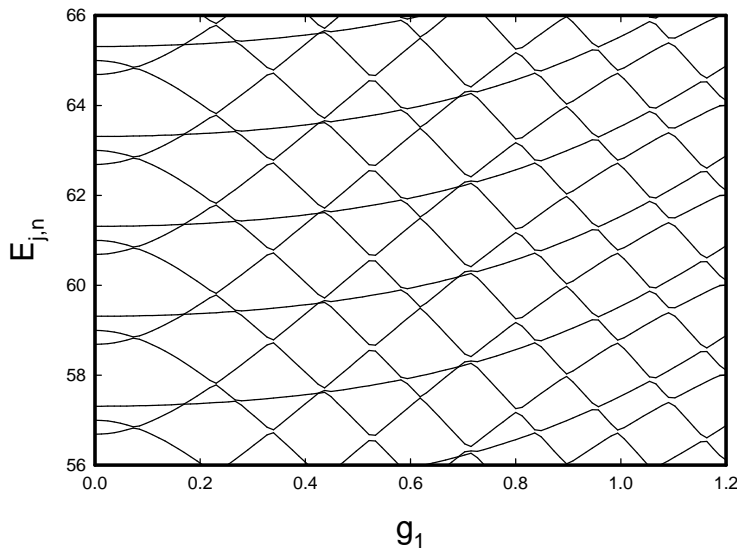


Figure 3. Energy levels as a function of g_1 for $g_2 = 1/3$ for even parity states, in the case of a model with $E_1 = 0$, $E_2 = 11 \hbar\omega_0$, and $E_3 = 24 \hbar\omega_0$, with $n_0 = 10^8$. The energy levels are in units of $\hbar\omega_0$, and are offset by $10^8 \hbar\omega_0$.

3. Energy levels away from anticrossings

To understand the systematics of the energy levels we consider solutions to the time-independent Schrödinger equation

$$E\Psi = \hat{H}\Psi \quad (9)$$

Some of the energy levels from such a computation are illustrated in Figure 3, where we have defined the dimensionless coupling strengths g_1 and g_2 according to

$$g_1 = \frac{U\sqrt{n}}{E_2 - E_1} \quad g_2 = \frac{V\sqrt{n}}{E_3 - E_2} \quad (10)$$

There are many energy levels; we expect three levels for each n , which is the same as we would get in the absence of coupling. As one can see from Figure 3, the complete spectrum is locally made up of three curves with the same pattern repeated over and over again with increasing energy (where the energy offset is $2 \hbar\omega_0$). The actual offset is $\hbar\omega_0$, but we have only included the even parity (even total index j plus n) energy levels to make the figure simpler. The energy levels of the odd parity (odd total index j plus n) are nearly identical, shifted by one unit of $\hbar\omega_0$. This periodicity occurs because in the large n limit, the coupling of $n + 1$ quanta is little different from coupling of n quanta. Under these conditions, the energy levels can be parameterized according to

$$E_{j,n}(g_1, g_2) = E_j(g_1, g_2) + n\hbar\omega_0 \quad (11)$$

The corresponding physical statement is that the oscillator impacts the three-level system strongly, causing the levels to shift; while the three-level system has very little impact on average on the oscillator, so that its levels are not shifted. This situation is similar to that observed in the spin-boson problem when n is large [24]. This motivates us to try to understand the shifted (or dressed) energy levels $E_j(g_1, g_2)$, as these are fundamental to the model in this limit.

3.1. Dressed energy levels from the rotated Hamiltonian \hat{H}_0

We can develop an effective estimate for the energy levels away from the anticrossings using an approach similar to that used for the spin-boson problem. We base our approximation on the eigenvalues of the rotated \hat{H}_0 problem which can be written as

$$\left(E + \frac{1}{2}\hbar\omega_0\right)\Phi = \begin{pmatrix} E_1(y) & 0 & 0 \\ 0 & E_2(y) & 0 \\ 0 & 0 & E_3(y) \end{pmatrix} + \frac{1}{2}\hbar\omega_0 \left(-\frac{d^2}{dy^2} + y^2\right)\Phi \quad (12)$$

We can separate the three-level degrees of freedom from the oscillator degree of freedom by using wavefunctions of the form

$$\Phi_{1,n} = \begin{pmatrix} 1 \\ 0 \\ 0 \end{pmatrix} u_1(y) \quad \Phi_{2,n} = \begin{pmatrix} 0 \\ 1 \\ 0 \end{pmatrix} u_2(y) \quad \Phi_{3,n} = \begin{pmatrix} 0 \\ 0 \\ 1 \end{pmatrix} u_3(y) \quad (13)$$

The $u_j(y)$ functions satisfy a one-dimensional Schrödinger equation of the form

$$\left(E + \frac{1}{2}\hbar\omega_0\right)u_j(y) = E_j(y) + \frac{1}{2}\hbar\omega_0 \left(-\frac{d^2}{dy^2} + y^2\right)u_j(y) \quad (14)$$

This is similar to what we obtained in the spin-boson problem [24].

3.2. Variational estimate

A useful approximation valued away from the level anticrossings can be developed by adopting trial wavefunctions in which the $u_j(y)$ function is taken to be a simple harmonic oscillator functions

$$u_j(y) = \phi_n(y) \quad (15)$$

Such a wavefunction is relevant in the large n limit for a variational estimate of the energy, leading to the approximation

$$E_{j,n}(g_1, g_2) = \langle n|E_j(y)|n\rangle + n\hbar\omega_0 = E_j(g_1, g_2) + n\hbar\omega_0 \quad (16)$$

Away from the anticrossings, the eigenfunctions of the original Hamiltonian \hat{H} have average n and j values which are close to the integer values which we assign in the rotated \hat{H}_0 problem here. When n is large, we can take advantage of the WKB approximation to write

$$\langle n | E_j(y) | n \rangle = \frac{1}{\pi} \int_{-\epsilon}^{\epsilon} \frac{E_j(y)}{\sqrt{\epsilon - y^2}} dy \quad (17)$$

with $\epsilon = 2n + 1$. When n is large, the WKB approximation gives excellent agreement with the results from a brute force solution of Equation (14), as was the case previously for the spin-boson problem. An algebraic expression in the case of the middle level is given in the Appendix.

4. Model test problem

To illustrate the approximation under discussion, we consider a specific example. In this example, we are interested in the basic question of whether the approximation described in the previous section is a good one away from resonance. However, since the three-level model and coupled oscillator problem is considerably more complicated than the analogous spin-boson problem, our task becomes more difficult. We focus on a three-level system with unperturbed energy splittings given by

$$E_2 - E_1 = 11 \hbar\omega_0 \quad E_3 - E_2 = 13 \hbar\omega_0 \quad (18)$$

with g_1 and ranging between 0 and 1, and g_2 ranging between 0 and 1.2 (we extend the range for g_2 since interesting features extend out a bit further along the g_2 axis).

4.1. Resonances associated with transitions between levels 1 and 2

We expect that the approximation for the energy levels discussed above will be best away from resonances, so our first goal is to understand where resonances occur. The most important resonances are those involving transitions between levels 1 and 2, and levels 2 and 3. In the case of resonances involving the lowest two levels, the resonance conditions is given approximately by

$$E_2(g_1, g_2) - E_1(g_1, g_2) = \Delta n \hbar\omega_0 \quad (19)$$

where Δn is odd. The associated contours are illustrated as a function of the dimensionless coupling constants g_1 and g_2 in Figure 4, based on the WKB approximation. When both g_1 and g_2 are small, it should take 11 oscillator quanta to match the transition energy since the energy levels in this case are only weakly perturbed. For small g_2 , the dressed transition energy $E_2(g_1, g_2) - E_1(g_1, g_2)$ increases with increasing g_1 , so that more oscillator quanta are required for a resonance. This can be seen in Figure 4 in the resonance contours for increasing Δn coming down to the g_1 axis. In the upper left of this figure, things are much more complicated. As g_2 increases, the splitting between the upper two levels is increased. If g_1 is small, then level 1 is only weakly coupled, and it is possible for level 2 to be pushed near level 1. The separation between the lower two levels is decreased, so that lower-order resonances (in which Δn is smaller) occur. The coupling due to the \hat{V} operator between the two lowest levels is much stronger for these lower-order resonances, so that the mixing is much greater and the associated level splitting is much larger. Approximating these states as pure

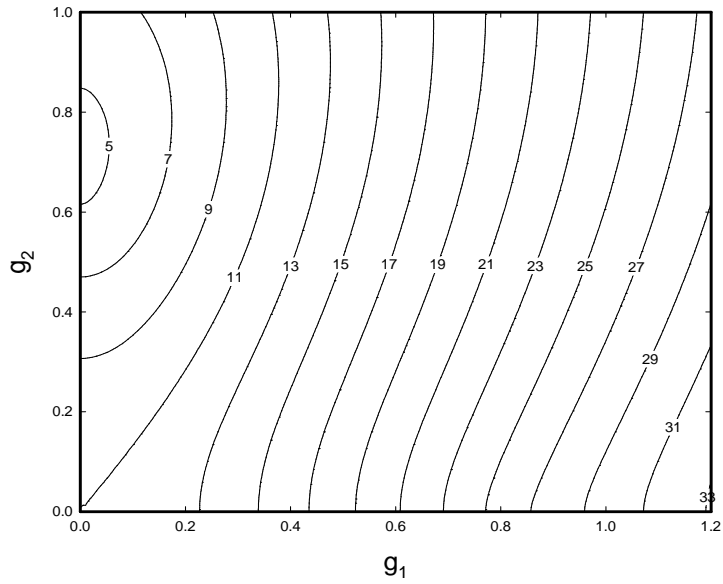


Figure 4. Contours for resonances between levels 2 and 1 (from the rotated \hat{H}_0 Hamiltonian), with the exchange of an odd number of oscillator quanta. The number of oscillator quanta Δn is indicated with each resonance.

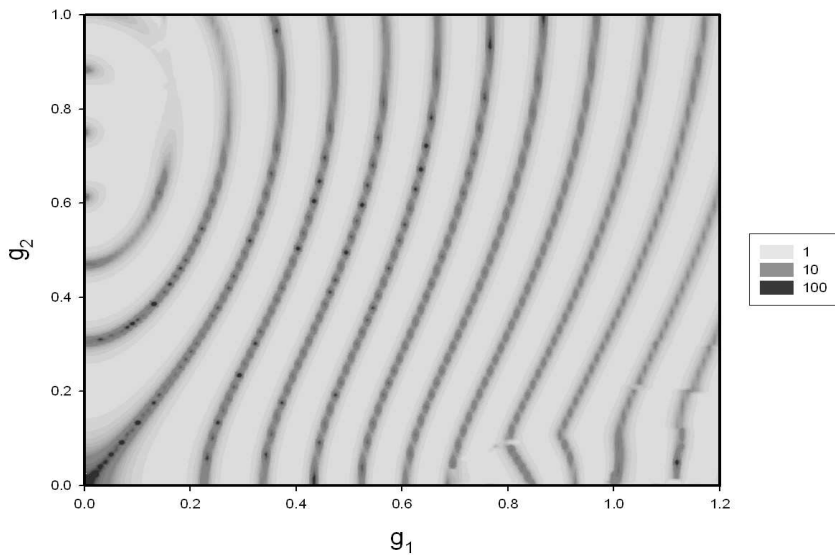


Figure 5. Resonances on transitions between levels 1 and 2 through the inverse magnitude of the resonance condition $|E_2(g_1, g_2) - E_1(g_1, g_2) - \Delta n \hbar \omega_0|^{-1}$ as a function of g_1 and g_2 . Computations for this plot are done using the original unrotated Hamiltonian \hat{H} . The results are in units of $(\hbar \omega_0)^{-1}$.

eigenfunctions of the \hat{H}_0 Hamiltonian becomes a much poorer approximation in this

regime.

We can see the resonances in the results shown in Figure 5 taken from a direct computation using the original \hat{H} Hamiltonian. One can see that most of the resonances predicted by the WKB approximation appear in the full computation.

4.2. Resonances associated with transitions between levels 2 and 3

The resonance condition associated with transitions between levels 2 and 3 is given approximately by

$$E_3(g_1, g_2) - E_2(g_1, g_2) = \Delta n \hbar \omega_0 \quad (20)$$

where once again the number of oscillator quanta exchanged must be odd. This resonance condition from WKB calculations is illustrated in Figure 6. For small g_1 and g_2 it now takes 13 oscillator quanta to match the transition energy, since in this case it is only weakly perturbed. When g_1 is small, an increase in g_2 pushes levels 2 and 3 apart, increasing the number of quanta required for a resonance. This situation is qualitatively similar as considered above, except that the axes are reversed. When g_2 is small, large values of g_1 can cause levels 1 and 2 to push apart strongly, driving level 2 toward level 3. Due to the asymmetry between the level splittings, this occurs for g_1 values larger than those for g_2 in the previous case for resonances between levels 1 and 2. The resulting small separation that occurs in the lower right hand part of Figure 6 between levels 2 and 3 leads to the occurrence of low-order resonances, with the associated strong mixing and large level shifts due to the \hat{V} operator.

Once again we show analogous results from direct calculations based on the original \hat{H} Hamiltonian in Figure 7. Most of the resonance lines from the WKB calculation are evident in the full \hat{H} calculation. The effects of the low-order resonances between levels 3 and 2 are apparent in the lower right part of the plot.

4.3. Energy levels

From the discussion above, we expect that the WKB energy level estimates based on the rotated Hamiltonian \hat{H}_0 should be good away from regions where resonances occur, and should be best where the separation between the nearest level is largest. In Figure 8 we illustrate the magnitude of the difference between the exact energies level 1 obtained from the original \hat{H} problem, and the WKB approximation:

$$\left| E_1(g_1, g_2) - \frac{1}{\pi} \int_{-\epsilon}^{\epsilon} \frac{E_1(y)}{\sqrt{\epsilon - y^2}} dy \right|$$

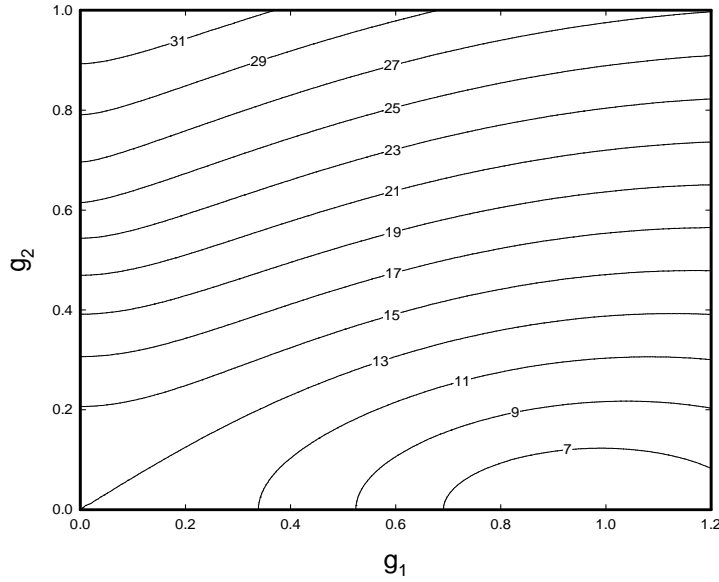


Figure 6. Contours for resonances between levels 3 and 2 (from the rotated \hat{H}_0 Hamiltonian), with the exchange of an odd number Δn of oscillator quanta. The contour labels indicate Δn .

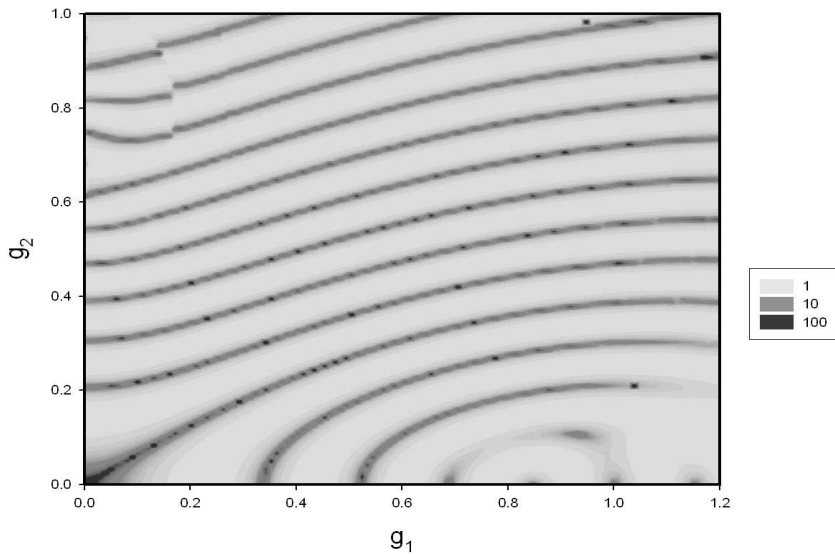


Figure 7. Resonances on transitions between levels 1 and 2 through the inverse magnitude of the resonance condition $|E_3(g_1, g_2) - E_2(g_1, g_2) - \Delta n \hbar \omega_0|^{-1}$ as a function of g_1 and g_2 . Computations for this plot are done using the original unrotated Hamiltonian \hat{H} . The results are in units of $(\hbar \omega_0)^{-1}$.

One sees that when g_1 and g_2 are small, that the difference is also small, and the approximation is very good. In the upper left part of the plot there occur the largest deviations as we expected due to low-order mixing effects not included in the \hat{H}_0

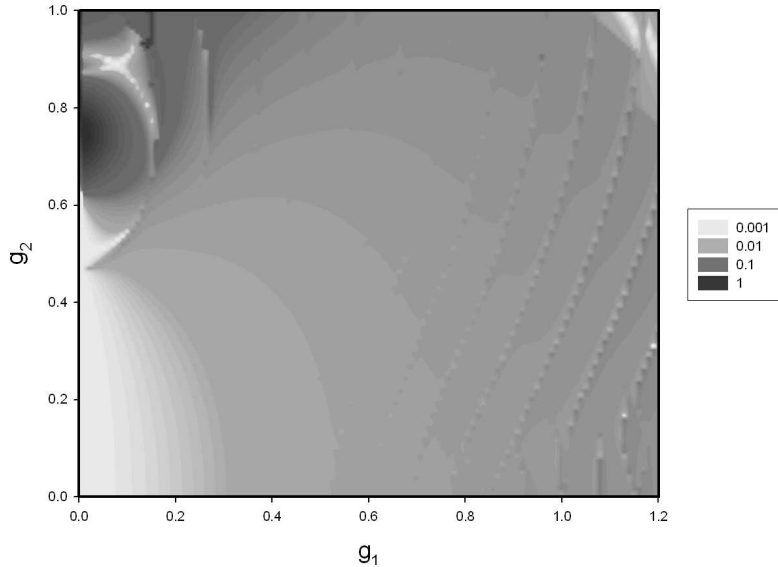


Figure 8. Magnitude of difference between the exact result for $E_1(g_1, g_2)$ from numerical calculations of the unperturbed Hamiltonian \hat{H} , and the WKB approximation for $E_1(g_1, g_2)$ in units of $\hbar\omega_0$.

problem. Elsewhere the agreement is generally rather good away from the resonances. The energy shift associated with the high-order resonances is not so large, and deviations are observable only when g_1 becomes large. We note that the energy level separation between the lowest two levels away from the upper left part of the plot is between about 10 and 40 $\hbar\omega_0$; hence the deviation between exact and approximate results is generally less than 0.1% of this separation. In the region where we would expect the approximation to be relevant, we find that it is very good.

In Figure 9 we show similar results for the magnitude of the difference in energy for level 3. Once again, the difference is small when g_1 and g_2 are small. Away from the lower right region (where level 2 is pushed toward level 3) the differences are small and the approximation is good. In the lower right region, strong mixing occurs due to the low-order resonances, and the approximation under discussion degrades.

In the case of level 2, the region where the approximation is accurate becomes further restricted, as can be seen in Figure 10. The strong mixing that we previously encountered in the upper left part of the plot in the case of level 1 is reproduced in the case of level 2, since level 1 is mixing primarily with level 2. The strong mixing associated with level 3 in the lower right part of the plot in the case of level 3 is also reproduced in the case of level 2, since level 3 is mixing with level 2 as well. Consequently, the best results are obtained in the central region, away from the problem regions in the upper

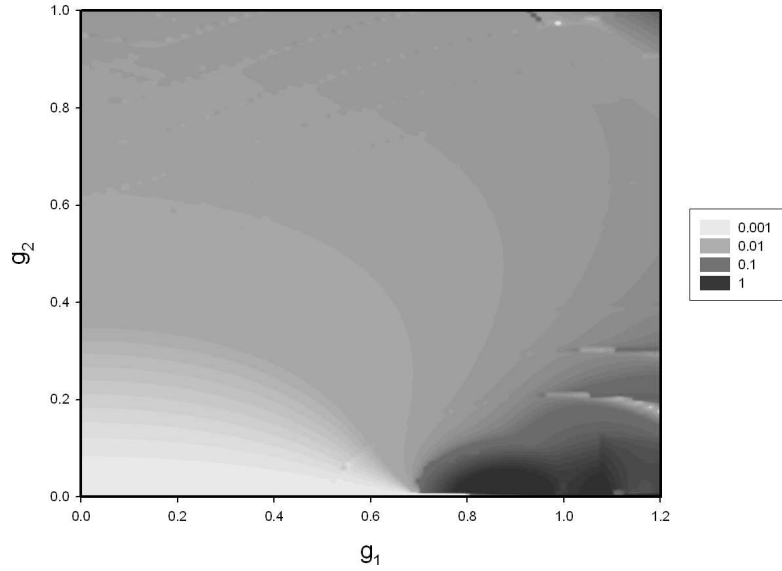


Figure 9. Magnitude of difference between the exact result for $E_3(g_1, g_2)$ from numerical calculations of the unperturbed Hamiltonian \hat{H} , and the WKB approximation for $E_3(g_1, g_2)$ in units of $\hbar\omega_0$.

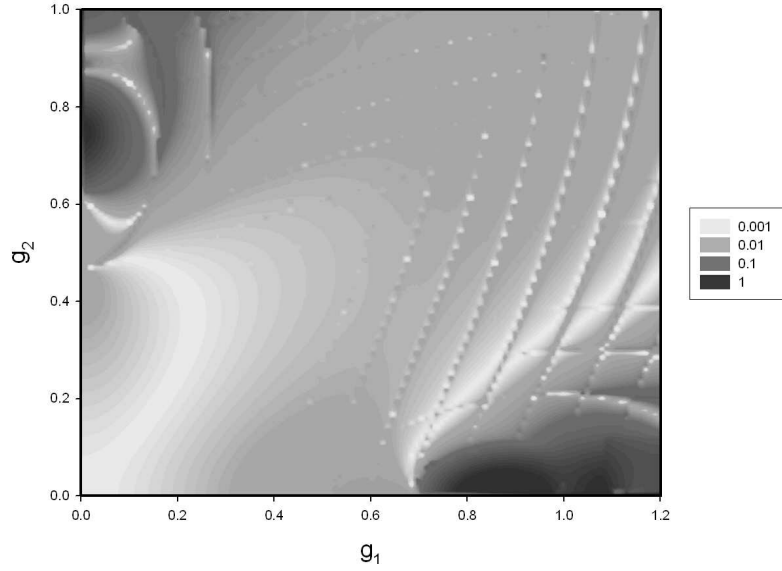


Figure 10. Magnitude of difference between the exact result for $E_2(g_1, g_2)$ from numerical calculations of the unperturbed Hamiltonian \hat{H} , and the WKB approximation for $E_2(g_1, g_2)$ in units of $\hbar\omega_0$.

left and lower right part of the region.

5. Remaining terms of the rotated Hamiltonian

We set out initially to implement a unitary transformation similar to the one which we studied previously in the spin-boson problem, in order to obtain a rotated Hamiltonian of the form

$$\hat{U}^\dagger \hat{H} \hat{U} = \hat{H}_0 + \hat{V} + \hat{W}$$

In previous sections we developed the first term in the rotated Hamiltonian \hat{H}_0 , and compared results from computations with those derived from the original Hamiltonian \hat{H} . To complete the unitary transformation, we need to rotate the simple harmonic oscillator part of the Hamiltonian to obtain \hat{V} and \hat{W} . We may write

$$\hat{V} + \hat{W} = \hat{U}^\dagger \left[\hbar\omega_0 \hat{a}^\dagger \hat{a} \right] \hat{U} - \hbar\omega_0 \hat{a}^\dagger \hat{a} \quad (21)$$

5.1. Transformation under rotation

Perhaps the simplest way to approach this problem is to examine how the simple harmonic oscillator operators transform under the unitary transform. The oscillator operators under discussion here are y , and $\frac{d}{dy}$, where

$$\frac{d}{dy} = \frac{\hat{a} - \hat{a}^\dagger}{\sqrt{2}}$$

Since the rotation diagonalizes the three-level system for each y , the unitary operators itself depends on y . We may write

$$\hat{U} = \hat{U}(y)$$

to exhibit this explicitly. There is no dependence of the unitary operator on $\frac{d}{dy}$. Consequently, the rotation of the oscillator operators can be written as

$$y' = \hat{U}^\dagger(y) y \hat{U}(y) = y \quad (22)$$

$$\frac{d}{dy'} = \hat{U}^\dagger(y) \frac{d}{dy} \hat{U}(y) = \frac{d}{dy} + \hat{U}^\dagger(y) \left[\frac{d}{dy} \hat{U}(y) \right] \quad (23)$$

5.2. Rotation of the harmonic oscillator

We can make use of this transformation to construct the other terms in the rotated Hamiltonian. We have

$$\hat{U}^\dagger \left[\hat{a}^\dagger \hat{a} \right] \hat{U} = \hat{U}^\dagger \left[\frac{1}{2} \left(y^2 - \frac{d^2}{dy^2} - 1 \right) \right] \hat{U} = \frac{1}{2} \left((y')^2 - \left[\frac{d}{dy'} \right]^2 - 1 \right) \quad (24)$$

Inserting expressions for the transformed operators produces

$$\begin{aligned} \hat{\mathcal{U}}^\dagger \left[\hat{a}^\dagger \hat{a} \right] \hat{\mathcal{U}} - \hat{a}^\dagger \hat{a} = \\ - \frac{1}{2} \left\{ \frac{d}{dy} \left[\hat{\mathcal{U}}^\dagger(y) \frac{d}{dy} \hat{\mathcal{U}}(y) \right] + \left[\hat{\mathcal{U}}^\dagger(y) \frac{d}{dy} \hat{\mathcal{U}}(y) \right] \frac{d}{dy} + \left[\hat{\mathcal{U}}^\dagger(y) \frac{d}{dy} \hat{\mathcal{U}}(y) \right]^2 \right\} \end{aligned} \quad (25)$$

This allows us to identify the two remaining parts of the rotated Hamiltonian, which we may write as

$$\hat{V} = - \frac{\hbar\omega_0}{2} \left\{ \frac{d}{dy} \left[\hat{\mathcal{U}}^\dagger(y) \frac{d}{dy} \hat{\mathcal{U}}(y) \right] + \left[\hat{\mathcal{U}}^\dagger(y) \frac{d}{dy} \hat{\mathcal{U}}(y) \right] \frac{d}{dy} \right\} \quad (26)$$

$$\hat{W} = - \frac{\hbar\omega_0}{2} \left[\hat{\mathcal{U}}^\dagger(y) \frac{d}{dy} \hat{\mathcal{U}}(y) \right]^2 \quad (27)$$

5.3. Reduction of $\hat{\mathcal{U}}^\dagger(y) \frac{d}{dy} \hat{\mathcal{U}}(y)$

It is possible to simplify these operators by taking advantage of properties of the unitary matrix. The unitary operator satisfies

$$\hat{\mathcal{U}}^\dagger(y) \hat{\mathcal{U}}(y) = 1 \quad (28)$$

independent of the parameter y . Hence, if we differentiate in y we obtain

$$\frac{d}{dy} \left[\hat{\mathcal{U}}^\dagger(y) \hat{\mathcal{U}}(y) \right] = \left[\frac{d}{dy} \hat{\mathcal{U}}^\dagger(y) \right] \hat{\mathcal{U}}(y) + \hat{\mathcal{U}}^\dagger(y) \left[\frac{d}{dy} \hat{\mathcal{U}}(y) \right] = 0 \quad (29)$$

A consequence of this is that the matrix which represents $\hat{\mathcal{U}}^\dagger(y) \frac{d}{dy} \hat{\mathcal{U}}(y)$ is antisymmetric if we chose $\mathcal{U}(y)$ to be a real matrix. In this case we may write

$$\begin{pmatrix} \mathcal{U}_{11} & \mathcal{U}_{21} & \mathcal{U}_{31} \\ \mathcal{U}_{12} & \mathcal{U}_{22} & \mathcal{U}_{32} \\ \mathcal{U}_{13} & \mathcal{U}_{23} & \mathcal{U}_{33} \end{pmatrix} \begin{pmatrix} \mathcal{U}'_{11} & \mathcal{U}'_{12} & \mathcal{U}'_{13} \\ \mathcal{U}'_{21} & \mathcal{U}'_{22} & \mathcal{U}'_{23} \\ \mathcal{U}'_{31} & \mathcal{U}'_{32} & \mathcal{U}'_{33} \end{pmatrix} = \begin{pmatrix} 0 & F_{12} & F_{13} \\ -F_{12} & 0 & F_{23} \\ -F_{13} & F_{23} & 0 \end{pmatrix} \quad (30)$$

where

$$\mathcal{U}'_{ij} = \frac{d}{dy} \mathcal{U}_{ij}(y)$$

The F_{ij} matrix elements can be obtained directly from the unitary matrix, which allows us to write

$$F_{12} = \mathcal{U}_{11}\mathcal{U}'_{12} + \mathcal{U}_{21}\mathcal{U}'_{22} + \mathcal{U}_{31}\mathcal{U}'_{32} \quad (31)$$

$$F_{23} = \mathcal{U}_{12}\mathcal{U}'_{13} + \mathcal{U}_{22}\mathcal{U}'_{23} + \mathcal{U}_{32}\mathcal{U}'_{33} \quad (32)$$

$$F_{13} = \mathcal{U}_{11}\mathcal{U}'_{13} + \mathcal{U}_{21}\mathcal{U}'_{23} + \mathcal{U}_{31}\mathcal{U}'_{33} \quad (33)$$

The $\hat{U}^\dagger(y)\frac{d}{dy}\hat{U}(y)$ operator can then be expanded as a sum of spatial parts and SU(3) matrices according to

$$\begin{aligned} \hat{U}^\dagger(y)\frac{d}{dy}\hat{U}(y) &= iF_{12}(y) \begin{pmatrix} 0 & -i & 0 \\ i & 0 & 0 \\ 0 & 0 & 0 \end{pmatrix} + iF_{13}(y) \begin{pmatrix} 0 & 0 & -i \\ 0 & 0 & 0 \\ i & 0 & 0 \end{pmatrix} \\ &\quad + iF_{23}(y) \begin{pmatrix} 0 & 0 & 0 \\ 0 & 0 & -i \\ 0 & i & 0 \end{pmatrix} \end{aligned} \quad (34)$$

5.4. Reduction of \hat{V}

We can use these results to recast the \hat{V} in a similar form. We may write

$$\begin{aligned} \hat{V} &= -i\frac{\hbar\omega_0}{2} \left\{ \left[\frac{d}{dy}F_{12}(y) + F_{12}(y)\frac{d}{dy} \right] \begin{pmatrix} 0 & -i & 0 \\ i & 0 & 0 \\ 0 & 0 & 0 \end{pmatrix} \right. \\ &\quad + \left[\frac{d}{dy}F_{13}(y) + F_{13}(y)\frac{d}{dy} \right] \begin{pmatrix} 0 & 0 & -i \\ 0 & 0 & 0 \\ i & 0 & 0 \end{pmatrix} \\ &\quad \left. + \left[\frac{d}{dy}F_{23}(y) + F_{23}(y)\frac{d}{dy} \right] \begin{pmatrix} 0 & 0 & 0 \\ 0 & 0 & -i \\ 0 & i & 0 \end{pmatrix} \right\} \end{aligned} \quad (35)$$

The \hat{V} operator written in this form is seen to be closely related to the one obtained in the spin-boson problem. A similar reduction of \hat{W} can be carried out without difficulty from these results.

6. Level splitting at the anticrossings

As discussed above, the energy levels away from the anticrossings are given approximately by

$$E_{j,n} = E_j(g_1, g_2) + n\hbar\omega_0$$

The approximate resonance conditions for the level anticrossings between the lowest two level as discussed above is

$$E_2(g_1, g_2) - E_1(g_1, g_2) = \Delta n \hbar\omega_0$$

for Δn odd. When we studied the rotated spin-boson system using a similar unitary transformation, we found that the level splitting was well approximated using degenerate perturbation theory in the rotated frame based on matrix elements of the \hat{V} operator. We expect a similar behavior in the three-level version of the problem, which would result in an estimate for the level splitting given by

$$\delta E = 2|\langle\Phi_{1,n}|\hat{V}|\Phi_{2,n-\Delta n}\rangle| \quad (36)$$

6.1. Level splittings, large Δn

As discussed in Section 4, the regions with different g_1 and g_2 would be expected to behave differently due to the presence of low-order resonances. Hence, we begin the discussion with a comparison in a relatively benign region in which levels 1 and 2 have large separation, and we stay away from the problem area in the lower right part of the plots discussed in Section 4. We seek resonances along a line with

$$g_2 = 0.3 g_1$$

Along this line the resonances between the lower two levels do not overlap other resonances; the resonances are all of high order, and there is no interference from the problem area associated with levels 2 and 3. Consequently we would expect the lower two levels to give good agreement, much as we found in the spin-boson problem with a two-level system. Results from computations based on the model test problem discussed in Section 4 are shown in Figure 11. We see in this figure very good agreement, similar to what we found in the spin-boson case [24].

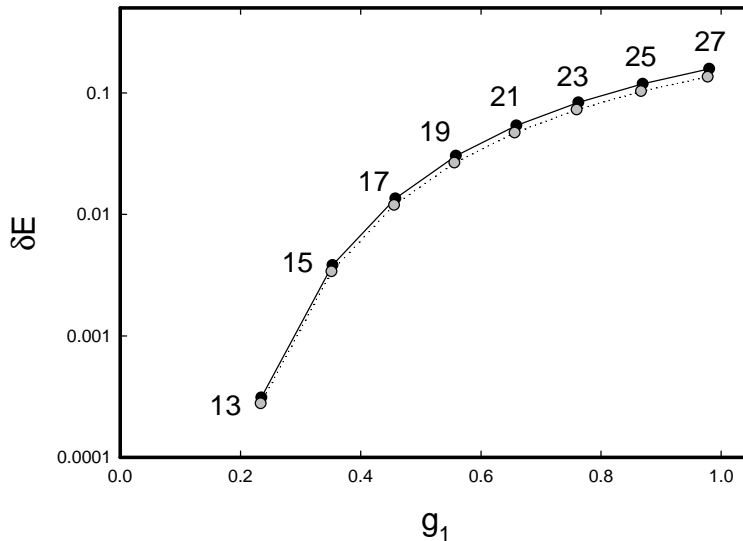


Figure 11. Level splitting at the anticrossings between levels 1 and 2 for the model described in Section 4, with $g_2 = 0.3g_1$. Black circles: degenerate perturbation theory based on wavefunctions in the rotated frame; gray circles: results from a direct computation using the original unrotated Hamiltonian \hat{H} . Energies are given in units of $\hbar\omega_0$.

6.2. Interaction with low-order resonances

We would expect a degradation of the approximation in the vicinity of the region where the other transition experiences low-order resonances. We continue to focus on the resonances involving the lowest two levels, this time on a line given by

$$g_2 = 0.1 g_1$$

which goes into the problem area with low-order transitions between the upper two levels. Results are presented in Figure 12. We see in this case good agreement between the results from degenerate perturbation theory based on the rotated problem, and results from the original \hat{H} problem everywhere except at resonances with Δn equal to 23 and 25. At these points the upper two levels are mixed due to strong low-order \hat{V} interactions, and one finds two resonances in the vicinity of the single resonance predicted by the rotated \hat{H}_0 model.

6.3. Other effects

We find poorer agreement when we move into the region in which g_2 is greater than g_1 . We consider in Figure 13 resonances along the line defined by

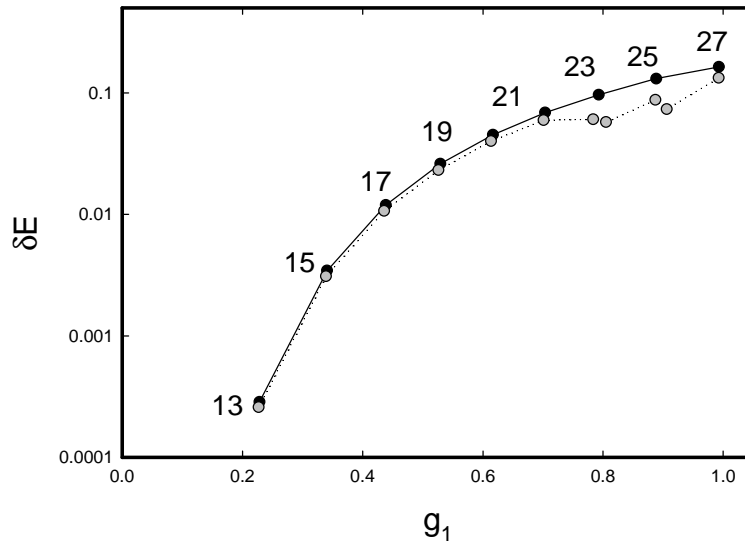


Figure 12. Level splitting at the anticrossings between levels 1 and 2 for the model described in Section 4, with $g_2 = 0.1g_1$. Black circles: degenerate perturbation theory based on wavefunctions in the rotated frame; gray circles: results from a direct computation using the original unrotated Hamiltonian \hat{H} . Energies are given in units of $\hbar\omega_0$.

$$g_2 = 1.1 g_1$$

The results in this case can be understood as being due to two different effects. The level splittings at the anticrossings for the full \hat{H} problem begin to fall systematically below those obtained from degenerate perturbation theory for the rotated problem once we consider the $g_2 = g_1$ line. Two of the resonances (13 and 17) are lower still due to interference from nearby resonances involving the upper two levels. We find poorer agreement between the exact numerical results for the \hat{H} problem and those from the approximation in this region, and worse still as the ratio of g_2 to g_1 increases further.

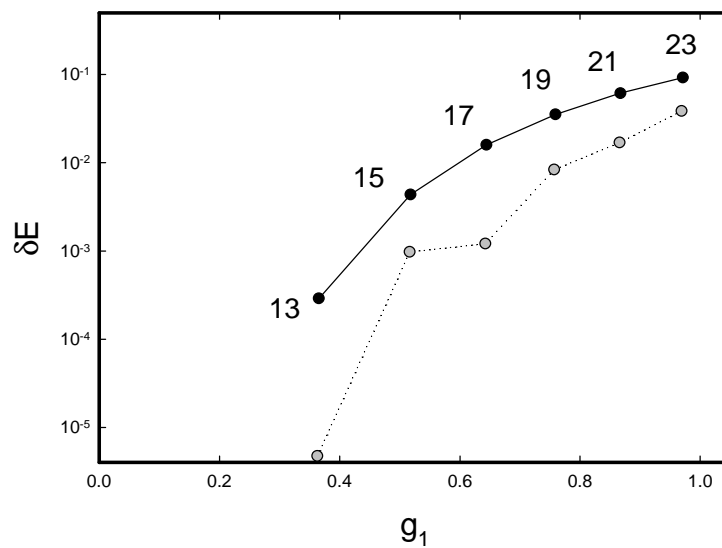


Figure 13. Level splitting at the anticrossings between levels 1 and 2 for the model described in Section 4, with $g_2 = 1.1g_1$. Black circles: degenerate perturbation theory based on wavefunctions in the rotated frame; gray circles: results from a direct computation using the original unrotated Hamiltonian \hat{H} . Energies are given in units of $\hbar\omega_0$.

7. Summary and conclusions

In our previous work, we considered the unitary transformation of the spin-boson problem which resulted in a rotated Hamiltonian that was functionally simpler (although more complicated mathematically). One part of the rotated Hamiltonian (\hat{H}_0) seemed to give rise to an underlying unperturbed problem in which the energy levels were very good, and in which no interaction was present between the different levels. Another part (\hat{V}) seemed to give a good account of the interaction responsible for the level splittings at the anticrossings. The remaining part (\hat{W}) is small in the large n limit, and could be neglected. In this work, we considered a generalization of the spin-boson model in which a three-level model is coupled to an oscillator. We were interested in whether a similar rotation could be developed, and whether it would exhibit similar useful properties. It was conjectured in Ref. [28] that the rotation could be applied to multilevel generalizations of the spin-boson problem, and the results presented here constitute such an example.

We succeeded in implementing such a rotation, which allowed us to develop analogous approximations for energy levels and for level splittings at the anticrossings. To study the approach, we developed a model test problem to provide a concrete example that could be used to compare results from numerically exact calculations with those from the rotated version of the problem. This model problem itself illustrated interesting new effects not present in the spin-boson problem, in which strong coupling between two levels result in one of the levels being pushed close to the third level. The resulting problem areas have no analog in the simpler spin-boson model.

The energy levels predicted from the rotated \hat{H}_0 problem are in excellent agreement with those of the full \hat{H} model away from the resonances, and away from the problem regions in the vicinity of low-order resonances. Approximate energy levels of the dressed problem were computed using the WKB approximation; which is convenient for numerical calculations, and which is in good agreement with energy levels obtained through brute force numerical solution of the \hat{H}_0 problem. Energy levels were generally found to be good to better than $0.1 \hbar\omega_0$ away from the problem regions, which corresponds to a relative accuracy of better than 0.1 % compared to the transition energies. The accuracy is similar to what is observed in the spin-boson problem for similar transition energies and dimensionless coupling strengths.

The computation of level splittings at the anticrossings requires the construction of interaction terms in the dressed problem, which is more difficult than in the spin-

boson problem because of complications due to the three-level model. We presented a straightforward method which relies on properties of the unitary transformation matrix, and can be implemented in practice relatively simply using numerical differentiation. Using these results, we found that the level splittings could be determined accurately using degenerate perturbation theory (similar to the case in the spin-boson problem); as long as the dimensionless coupling strength (g_1 or g_2) of the transition in question was the larger of the two, and as long as computations are done away from the problem area with low-order resonances on the other transition. We expect that improved results for the level splittings can be obtained by employing somewhat more sophisticated approximations than first-order degenerate perturbation theory. Few-state models in the rotated frame that take into account interfering resonances would be expected to extend the range over which the level splittings could be approximated accurately.

The dressed problem resulting from the unitary transformation provides a different view of the coupled three-level and oscillator problem which allows us to understand the multiphoton regime. The new energy level approximation seems to work well, and may be useful for applications. The approximation for calculating level splittings is less robust, but also seems to be useful as long as applied in trouble-free regions. We would expect this approach to apply to more complicated models involving more levels, which would provide similar predictive capability for state energies. In general, the approach should be most useful in regimes in which the oscillator energy is small compared to all relevant transition energies.

Appendix A. Solution of the eigenvalue equation

The characteristic equation for the energy eigenvalues that we obtained in the diagonalization of the three-level system is the cubic equation

$$(E_1 - E)(E_2 - E)(E_3 - E) - (E_1 - E)2V^2y^2 - (E_3 - E)2U^2y^2 = 0$$

In this Appendix, we review the solution for the three energy eigenvalues (the solutions of which are well known, but not usually presented in the form we discuss). Our strategy will be to reduce it to the form of the triple angle sine formula

$$4 \sin^3 \frac{\theta}{3} - 3 \sin \frac{\theta}{3} = -\sin \theta \quad (\text{A.1})$$

Appendix A.1. Offset

We first define a new energy variable that is offset by the average energy of the three states

$$\epsilon = E - \frac{E_1 + E_2 + E_3}{3} \quad (\text{A.2})$$

which allows us to rewrite the characteristic equation in the form

$$\epsilon^3 - \alpha\epsilon = \beta \quad (\text{A.3})$$

where α and β are given by

$$\alpha = \frac{E_1^2 + E_2^2 + E_3^2 - E_1E_2 - E_1E_3 - E_2E_3}{3} + 2U^2y^2 + 2V^2y^2 \quad (\text{A.4})$$

$$\begin{aligned} \beta = & \frac{2}{27}(E_1^3 + E_2^3 + E_3^3) - \frac{1}{9}[E_1^2(E_2 + E_3) + E_2^2(E_1 + E_3) + E_3^2(E_1 + E_2)] \\ & + \frac{4}{9}E_1E_2E_3 + \frac{2}{3}U^2y^2(E_1 + E_2 - 2E_3) + \frac{2}{3}V^2y^2(E_2 + E_3 - 2E_1) \end{aligned} \quad (\text{A.5})$$

Appendix A.2. Scaling

Next, we scale according to

$$\epsilon = A \sin \frac{\theta}{3} \quad (\text{A.6})$$

This leads to

$$4 \sin^3 \frac{\theta}{3} - \frac{4\alpha}{A^2} \sin \frac{\theta}{3} = \frac{4\beta}{A^3} \quad (\text{A.7})$$

The triple angle sine formula is recovered with the identifications

$$\frac{4\alpha}{A^2} = 3 \quad (\text{A.8})$$

$$\frac{4\beta}{A^3} = -\sin \theta \quad (\text{A.9})$$

Appendix A.3. Energy eigenvalues

Since the sine function is invariant under shifts of multiples of 2π

$$\sin \theta = \sin(\theta + 2\pi) = \sin(\theta + 4\pi) \quad (\text{A.10})$$

there are three solutions to the triple angle sin formula

$$\sin\left(\frac{\theta}{3}\right), \sin\left(\frac{\theta + 2\pi}{3}\right), \sin\left(\frac{\theta + 4\pi}{3}\right)$$

Consequently, we obtain three solutions to the eigenvalue equation which we may write as

$$E = \frac{E_1 + E_2 + E_3}{3} + A \sin\left(\frac{\theta}{3}\right) \quad (\text{A.11})$$

$$E = \frac{E_1 + E_2 + E_3}{3} + A \sin\left(\frac{\theta + 2\pi}{3}\right) \quad (\text{A.12})$$

$$E = \frac{E_1 + E_2 + E_3}{3} + A \sin\left(\frac{\theta + 4\pi}{3}\right) \quad (\text{A.13})$$

with

$$A = \sqrt{\frac{4\alpha}{3}} \quad (\text{A.14})$$

$$\theta = \arcsin\left(-\frac{4\beta}{A^3}\right) \quad (\text{A.15})$$

The first of these energy expressions evaluates to the middle value of E_1 , E_2 , and E_3 when $y = 0$. When $y = 0$, the second evaluates to the maximum of E_1 , E_2 , and E_3 , and the third expression evaluates to the minimum of the three unperturbed energies.

Appendix A.4. Algebraic expressions are inconvenient

It is possible to develop algebraic expressions by taking advantage of the addition formula

$$\sin(a + b) = \sin a \cos b + \cos a \sin b \quad (\text{A.16})$$

The energy eigenvalues then can be written as

$$E = \frac{E_1 + E_2 + E_3}{3} + A \sin\left(\frac{\theta}{3}\right) \quad (\text{A.17})$$

$$E = \frac{E_1 + E_2 + E_3}{3} + A \left[-\frac{1}{2} \sin\left(\frac{\theta}{3}\right) + \frac{\sqrt{3}}{2} \cos\left(\frac{\theta}{3}\right) \right] \quad (\text{A.18})$$

$$E = \frac{E_1 + E_2 + E_3}{3} + A \left[-\frac{1}{2} \sin\left(\frac{\theta}{3}\right) - \frac{\sqrt{3}}{2} \cos\left(\frac{\theta}{3}\right) \right] \quad (\text{A.19})$$

To proceed, we require explicit expressions for $\sin(\theta/3)$ and $\cos(\theta/3)$. We begin by writing for $\sin \theta$

$$\sin \theta = \frac{e^{i\theta} - e^{-i\theta}}{2i} = -\frac{3^{\frac{3}{2}}\beta}{2\alpha^{\frac{3}{2}}} \quad (\text{A.20})$$

We can solve for $e^{i\theta}$ to obtain

$$e^{i\theta} = -i \frac{3^{\frac{3}{2}}\beta}{2\alpha^{\frac{3}{2}}} \pm \sqrt{1 - \frac{27\beta^2}{4\alpha^3}} \quad (\text{A.21})$$

Either choice of sign is acceptable, but we will choose a + sign for what follows. This allows us to write

$$\sin\left(\frac{\theta}{3}\right) = \frac{1}{2i} \left\{ \left[\sqrt{1 - \frac{27\beta^2}{4\alpha^3}} - i \frac{3^{\frac{3}{2}}\beta}{2\alpha^{\frac{3}{2}}} \right]^{\frac{1}{3}} - \left[\sqrt{1 - \frac{27\beta^2}{4\alpha^3}} - i \frac{3^{\frac{3}{2}}\beta}{2\alpha^{\frac{3}{2}}} \right]^{-\frac{1}{3}} \right\} \quad (\text{A.22})$$

$$\cos\left(\frac{\theta}{3}\right) = \frac{1}{2} \left\{ \left[\sqrt{1 - \frac{27\beta^2}{4\alpha^3}} - i \frac{3^{\frac{3}{2}}\beta}{2\alpha^{\frac{3}{2}}} \right]^{\frac{1}{3}} + \left[\sqrt{1 - \frac{27\beta^2}{4\alpha^3}} - i \frac{3^{\frac{3}{2}}\beta}{2\alpha^{\frac{3}{2}}} \right]^{-\frac{1}{3}} \right\} \quad (\text{A.23})$$

Unfortunately, these expressions are complicated in a way that makes them inconvenient for calculations.

Appendix A.5. Analytic WKB expression

It is possible to use these results to develop analytic expressions for the WKB approximation for the energy levels discussed in Section 3. In the case of the middle level, we may write the approximation as

$$E_2(g_1, g_2) = \frac{1}{\pi} \int_{-\epsilon}^{\epsilon} \frac{E_2(y)}{\sqrt{\epsilon - y^2}} dy \quad (\text{A.24})$$

After substituting in for $E_2(y)$ we obtain

$$E_2(g_1, g_2) = \frac{E_1 + E_2 + E_3}{3} + \frac{1}{\pi} \int_{-\epsilon}^{\epsilon} \frac{A(y) \sin\left(\frac{1}{3} \arcsin\left[-\frac{4\beta(y)}{A^3(y)}\right]\right)}{\sqrt{\epsilon - y^2}} dy \quad (\text{A.25})$$

Similar analytic expressions can be written for the other two levels directly.

References

- [1] Bloch F and Siegert A 1940 *Phys. Rev.* **57** 522
- [2] Shirley J 1965 *Phys. Rev.* **138**, B979
- [3] Cohen-Tannoudji C, Dupont-Roc J, and Fabre C 1973 *J. Phys. B: At. Mol. Phys.* **6** L214
- [4] Pegg D T 1973 *J. Phys. B: At. Mol. Phys.* **6** 246
- [5] Ahmad F and Bullough R K 1974 *J. Phys. B: At. Mol. Phys.* **7** L275
- [6] Hattori T and Kobayashi T *Phys. Rev. A* **35** 2733
- [7] Førre M 2004 *Phys. Rev. A* **70** 013406
- [8] Ostrovsky V N and Horsdal-Pedersen E 2004 *Phys. Rev. A* **70** 033413
- [9] Graham H and Höhnerbach M 1984 *Z. Phys. B* 233
- [10] Ciblis M B *et al* 1991 *J. Phys. A: Math. Gen.* **24** 1661
- [11] Wang K, Ho T and Chu I 1985 *J. Phys. B: At. Mol. Phys.* **18** 4539
- [12] D'Andrea A *Phys. Rev. A* **39** 5143
- [13] Matisov B, Mazets I and Windholz L 1995 *Quantum Semiclass. Opt.* **7** 449
- [14] Liu Z, Lin Y, Shang K and Zeng L 1999 *Physics Letters A* **264** 137
- [15] Klimov A B, Sainz I, and Chumakov S M 2003 *Phys. Rev. A* **68** 063811
- [16] Radmore P M and Knight P L 1981 *J. Phys. B: At. Mol. Phys.* **15** 561
- [17] Li X, Lin D L and Gong C 1987 *Phys. Rev. A* **36** 5209
- [18] Cardimona D A 1990 *Phys. Rev. A* **41** 5016
- [19] Wu Y and Yang X 1997 *Phys. Rev. A* **56** 2443
- [20] Klimov A B, Sánchez-Soto L L, Navaroo A and Yustas E C 2002 *J. Mod. Optic.* **49** 2211
- [21] Bougouffa S and Kamli A 2004 *J. Opt. B. Quantum Semiclass. Opt.* **6** S60
- [22] Abdel-Wahab N H 2007 *Phys. Scr.* **76** 244
- [23] Georgi H 1999 *Lie Algebras in Particle Physics* (New York:Perseus Books) p 98
- [24] Hagelstein P L and Chaudhary I U, to appear in *J. Phys. B*; available as *Preprint quant-ph/0709.1961*
- [25] Hagelstein P L and Chaudhary I U, to appear in *J. Phys. B*; available as *Preprint quant-ph/0709.3557*
- [26] Wagner M 1979, *Zeit. für Physik B* **32** 225
- [27] Yoo H I and Eberly J H 1985 *Physics Reports* **118** 239
- [28] Larson J and Stenholm S 2006 *Phys. Rev. A* **73** 033805